ELSEVIER

Remote Sensing of Environment 82 (2002) 79–94

Remote Sensing of Environment

www.elsevier.com/locate/rse

Validation of empirical SeaWiFS algorithms for chlorophyll-*a* retrieval in the Mediterranean Sea A case study for oligotrophic seas

Fabrizio D'Ortenzio [a,*], Salvatore Marullo [b], Maria Ragni [a], Maurizio Ribera d'Alcalà [a], Rosalia Santoleri [c]

[a]*Laboratorio di Oceanografia Biologica, Stazione Zoologica Napoli "A. Dohrn", Villa Comunale, Naples, Italy*
[b]*Ente Nazionale per le nuove tecnologie l'Energia e l'Ambiente, ENEA, Centro Ricerche Casaccia, Rome, Italy*
[c]*Istitituto di Fisica Dell'Atmosfera, CNR, Rome, Italy*

Received 9 October 2000; received in revised form 12 December 2001; accepted 11 January 2002

Abstract

The major aim of this paper is the validation of SeaWiFS-derived chlorophyll-*a* concentration in the Mediterranean Sea. A data set containing in situ chlorophyll-*a* profiles and optical measurements of in-water and above-water radiances was used to evaluate the performances of several ocean color algorithms in the Mediterranean Sea. The analysis revealed a systematic overestimation of chlorophyll-*a* concentration by National Aeronautics and Space Administration (NASA) global algorithms (OC2v4 and OC4v4). The error appears to be correlated with chlorophyll-*a* concentration, by exhibiting marked differences at low values ($C < 0.15$ mg/m^3). In particular at low concentration, the bias observed for OC2v4 is about twice that observed for OC4v4. The same analysis made using the Gitelson et al. [J. Mar. Syst. 9 (1996) 283.] Coastal Zone Color Scanner (CZCS) regional algorithm (GIT) revealed that this model underestimates the pigments concentration but it does not exhibit a correlation between the error and the measures. On the other hand, when the NASA standard algorithms are applied to remotely sensed data, the behavior appears reversed: the OC2v4 algorithm exhibits better estimates than OC4v4, which is probably more affected by atmospheric correction problems. When applied to satellite data, the GIT algorithm performs better than the NASA global algorithms, although the estimates are very poor in the high chlorophyll-*a* range. Two new Mediterranean algorithms are then proposed by fitting our Mediterranean bio-optical data set with linear and OC2-like functional forms. The new algorithms perform well when applied either to the bio-optical measurements or to satellite data. The different behavior of the same algorithm when applied to bio-optical measurements or to remotely sensed data demonstrates that the atmospheric correction is still the main source of error in ocean color data. Due to the relatively small number of available in situ data, the algorithms that we generated have to be considered very preliminary. Discussion was carried out on the reasons of the global algorithm misfit, providing possible explanations and some preliminary result. The influence of coccolithophores and of the yellow substance on the optical response of the Mediterranean waters is investigated, showing that they can at least partially explain the systematic misfit. All the above shows that a region like the Mediterranean Sea requires an independent treatment of the atmospheric and of the in-water bio-optical term to obtain reliable estimates of phytoplankton activity.

1. Introduction

The quantification of the spatial and time variability of phytoplankton biomass and biological activity is among the main scopes of ocean color observation missions. The Coastal Zone Color Scanner (CZCS) mission produced between 1978 and 1986 an invaluable new set of ocean color data that substantially contributed to increase information on a large variety of biological processes (Gregg & Conkright, 2001; Harris, Feldman, & Griffiths, 1993; Yentsch, 1993; Yoder, McClain, Feldman, & Esaias, 1993). Moreover, the CZCS mission demonstrated also the potentiality of ocean color data to characterize the dynamical features and the variability of the ocean circulation pattern from mesoscale to large scale (see Abbott & Chelton, 1991, for a review). The scientific success of the CZCS

* Corresponding author. Tel.: +39-81-5833-201; fax: +39-81-5833-224.
E-mail address: fadorte@alpha.szn.it (F. D'Ortenzio).

0034-4257/02/$ - see front matter
PII: S0034-4257(02)00026-3

mission induced the space agencies to develop a new generation of ocean color sensors. Among these, the National Aeronautics and Space Administration (NASA) launched in September 1997 the still operating SeaStar satellite mounting on board SeaWiFS sensor and recently the Terra Satellite with the MOderate Resolution Imaging Spectroradiometer (MODIS) sensor; the European Space Agency (ESA) developed the MEdium-Resolution Imaging Spectrometer (MERIS) that will be launched at the beginning of 2002. This new generation of sensors is characterized by more detailed spectral information, higher spectral resolution, better calibration stability than the CZCS, and provides for the first time a global ocean daily coverage (Barnes, Pagano, & Salomonson, 1998; Doerffer, Sorensen, & Aiken, 1999; Hooker, McClain, & Holmes, 1993; McClain & Fargion, 1999; Rast & Bezy, 1999).

At the same time, a parallel effort in the improvement of bio-optical and atmospheric correction algorithms has been carried out (Carder, Chen, Lee, Hawes, & Kamykowski, 1999; Esaias et al., 1998; Gordon & Wang, 1994; Hooker & McClain, 2000; McClain et al., 1992; Moore, Aiken, & Lavender, 1999; O'Reilly et al., 2000; Wang, 2000).

One of the main aims of the SeaWiFS Project is to obtain valid ocean color data of the world ocean with an uncertainty of 5% in the determination of the water leaving radiances in clear-water regions and an uncertainty within ± 35% in the estimation of the chlorophyll-*a* concentrations over the range 0.05–50 mg/m^3 for Case 1 waters (Hooker & McClain, 2000).

Most of the bio-optical algorithms estimating chlorophyll-*a* or total pigment concentration (chlorophyll-*a* + phaeopigments) from ocean radiance data have been empirically derived. This is the case of the OC2 algorithm, described by O'Reilly et al. (1998), and initially used by NASA in the operational processing of SeaWiFS data. OC2 estimates chlorophyll-*a* concentration for Case 1 waters as function of the ratio between remote sensing reflectances at 490 and 555 nm, using coefficients derived by a statistical fit with SeaBASS (SeaWiFS Bio-optical Archive and Storage System) data (see O'Reilly et al., 1998, for a description). In the same paper, they also proposed a four-band algorithm (OC4). Subsequent analysis indicated that OC2 could be biased when applied to specific regions. Kahru and Mitchell (1999) showed that OC2 overestimates chlorophyll-*a* at high concentrations in the California Current area. For this reason, they proposed a new regional version of the algorithm based on a fit with CalCOFI (California Cooperative Oceanic Fisheries Investigation) data. In a recent review paper, describing the main results of calibration and validation activity performed in the framework of SeaWiFS Project, Hooker and McClain (2000) showed that chlorophyll-*a* retrievals are within the accuracy goals stated above for the Case 1 waters for most of the data. Nevertheless, the same authors found that for very low (< 0.3 mg/m^3) and high (> 3 mg/m^3) chlorophyll-*a* concentrations, the satellite overestimates the in situ-measured values.

Recently, in the framework of several research programs (ENVISAT Cal-Val Team, 2000; Fargion & McClain, 2000) specifically devoted to the calibration and validation of ocean color sensors, a large amount of in situ measurements have been collected. These new data increased their total amount. Using this larger data set, O'Reilly et al. (2000) proposed an updated version of the ocean chlorophyll-*a* two- (OC2v4) and four-band (OC4v4) algorithms. They suggested that the OC4v4 is expected to perform better than OC2v4 when applied to satellite-derived water leaving radiances both in oligotrophic and eutrophic conditions. Subsequently, NASA adopted OC4v4 algorithm for the global SeaWiFS processing.

Empirical regression-based algorithms obviously perform well when pigment composition of phytoplankton is similar to that of the samples used to generate the algorithm. Global algorithms (i.e., OC4v4) have to reflect average pigment composition at global scale and, due to the significant variation of pigment composition of specific phyto assemblages in different regions of the oceans, they tend to be overspread. Regional algorithms, fitted to local biological characteristics generally perform better, and appear to be very promising to reach the SeaWiFS project requirements in particular areas.

Differences in the performance of regional and global algorithms might be also enhanced by peculiarities in the atmospheric term (Dierssen & Smith, 2000; Jorgensen, 1999; Kahru & Mitchell, 1999; Léon, Chazette, & Dulac, 1999), which indeed affect radiances and the result is important in a misfit of the algorithm.

Since the Mediterranean Sea is one of the most relevant regional seas in the world, we aimed to validate ocean color algorithms in this area, with a particular attention to those operationally used in the SeaWiFS data processing. Moreover, the Mediterranean exhibits a general oligotrophic regime characterized by surface chlorophyll-*a* values usually less than 0.3 (Antoine, Morel, & André, 1995; Morel & André, 1991), i.e., in the range in which the available SeaWiFS algorithms have already revealed their limits (Hooker & McClain, 2000). Ocean color data, if properly validated, may result an invaluable information to understand the functioning of the basin.

The paper is organized as follows: we first outline the main features of the area and report of existing regional algorithms (Section 2.1); then we describe the composition of the data set and the methods used to collect and process it (Sections 2.2 and 2.3). Satellite data processing and acquisition methods are described in Section 2.4. The results of the validation of selected empirical algorithms (Section 3.1) are reported in Section 3.2. Section 3.3 describes a new set of coefficients derived for a Mediterranean algorithm. In Section 3.4, the algorithms tested in the previous section are applied to satellite data and validated. In Section 4, we discuss the results of the validation underlining open questions and possible answers. Finally, in the last section, we summarize the results.

2. Study area, data, and methods

2.1. Study area

The Mediterranean Sea is a mid-latitude, predominantly oligotrophic and ultra-oligotrophic basin. However, higher biomass may locally and seasonally occur in regions affected by river runoff or by deep convection events (Antoine et al., 1995). This basin is a good oceanographic test area both for its complex ocean dynamics, which mimics several basic processes of ocean functioning and for its intensive anthropogenic pressure.

The Mediterranean area is strongly affected by industrial emissions from the northern border and desert dust from the south. Aerosols transported to the Mediterranean Sea may be considered to consist of anthropogenic-rich "background" materials supplied continuously from Europe, upon which sporadic pulses of Saharan crust-rich dust are superimposed. Schematically, the latter represent more than 90% of the mass of particulate atmospheric deposition, though they occur 10% of the time in the Mediterranean atmosphere, whereas the inverse figures apply to anthropogenic aerosols (Gilman & Garrett, 1994). Despite high interannual variability, the dust exported from Africa over the Mediterranean is higher in the eastern Mediterranean in spring and spreads over the western Mediterranean in summer (Guerzoni, Molinaroli, & Chester, 1997; Prospero, 1996). The very peculiar aerosol composition makes more difficult the use of routine remote sensing procedures for atmospheric correction (Moulin, Dulac, et al., 1997; Moulin, Guillard, Dulac, & Lambert, 1997).

Furthermore, previous study on CZCS data in this basin (Antoine et al., 1995; Morel & André, 1991) showed that the global ocean color bio-optical algorithm often results in a poor estimate of the chlorophyll-*a*. All the considerations above imply the need of a special validation effort for the Mediterranean Sea and eventually the development of new regional ocean color algorithms (Barale & Schlittenhardt, 1993).

Gitelson, Karnieli, Goldman, Yacobi, and Mayo (1996) showed that the CZCS global algorithm (Gordon & Morel, 1983) overestimates the observed pigment concentrations in the eastern Mediterranean Sea. They proposed a region-specific empirical algorithm to derive pigment concentrations from CZCS images on the basis of a limited number of measurements (21 stations), collected off the Israeli coast (eastern Mediterranean) in June 1992. Even if this algorithm can be considered a regional algorithm, its general applicability to the Mediterranean Sea is limited by the small number of data used for the regression and the limited area and period (only 1 day) of the in situ measurements.

In view of the SeaWiFS ocean color algorithms' validation in the Mediterranean Sea, a specific data set of bio-optical and pigment concentration measurements has been built during the period 1998–2000 in the framework of the SYMPLEX (SYnoptic Mesoscale and PLankton EXperiment) Project of the Italian Space Agency (ASI). This data set is used in this paper for the validation of the most widely used chlorophyll-*a* algorithms and to retrieve a first version of a regional algorithm for the Mediterranean.

2.2. In situ chlorophyll-a data

In situ chlorophyll-*a* measurements were performed during three cruises carried out in the Mediterranean Sea through the years 1999–2000 on board the R/V *Urania* of the National Research Council (CNR). The activity was mostly sponsored by the ASI in the framework of its support to basic research aimed at validating remote observations of the Earth. The locations of the stations are reported in Fig. 1a. Coastal stations were excluded from the data set in order to avoid Case 2 water properties.

During each cruise, water samples were taken from Niskin bottles mounted on a General Oceanics Rosette equipped with an SBE 911 CTD profiler and a SeaTech fluorometer. Subsamples to measure chlorophyll-*a* (C) and phaeophytin-*a* (P) were filtered on board on GF/F filters (low *vacuum*) and immediately deep-frozen. Pigment concentrations were subsequently determined at the Stazione Zoologica di Napoli "A. Dohrn" (SZN) on 90% acetone extracts within few weeks of the sampling using a SPEX Fluorolog spectrofluorometer with an estimated coefficient of variation for chlorophyll-*a* concentration of ~10% (Neveux & Panouse, 1987).

For each cruise, we merged and linearly fitted spectrofluorometrically derived chlorophyll-*a* concentrations with data acquired by the SeaTech in situ fluorometer. Therefore, the data set consists of 582 chlorophyll-*a* profiles derived from the calibrated fluorescence profiles. Additional data were extracted from the data set of the Dynamique des Flux de mAtière en MEDiterranée (DYFAMED) station located in the Ligurian basin (Marty, Chiaverini, La Rosa, & Miquel, 1995 and Fig. 1a). The data are available on the World Wide Web (http://www.obs-vlfr.fr/jgofs2/sodyf/home.htm).

For the stations where phaeophytin-*a* concentrations were not available (e.g., DYFAMED), we estimated the total concentration of chlorophyll-*a* + phaeopigments ($C+P$), using a linear fit of C versus $C+P$, following an approach very similar to O'Reilly et al. (1998). This fit was based on 798 data points derived from the reported cruises and 7 additional ones conducted in the Mediterranean during the years 1995–2000 by the SZN group, and gave the following equation:

$$C + P = 1.1635C + 0.0072 \tag{2.1}$$

with a correlation coefficient of R^2=.997.

Eq. (2.1) was then used to obtain total pigment concentration profiles in those stations where only chlorophyll-*a* was available.

The final data set covers a relatively wide range of conditions in Case 1 waters of the Mediterranean Sea, spanning

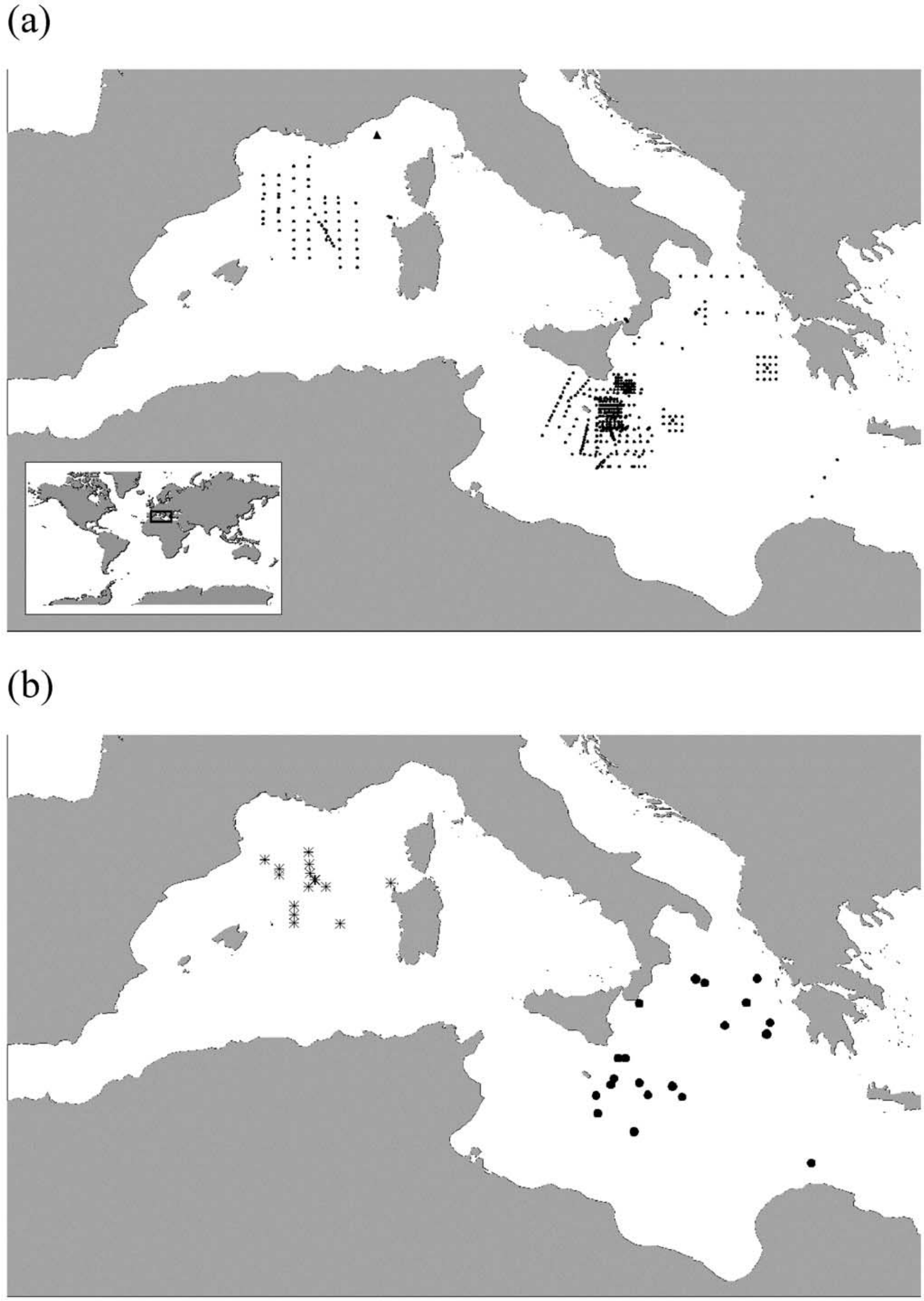

Fig. 1. The Mediterranean Sea. (a) The location of in situ chlorophyll-*a* profiles are reported. Dots refer to SYMPLEX cruises. Triangle indicates the DYFAMED location. (b) Location of concurrent bio-optical measurements and chlorophyll-*a* profiles. Stars indicate the SIMBAD measurements, dots the SPMR Satlantic measurements.

from oligotrophic (Sicily Channel and Ionian Sea) to moderately eutrophic regimes (northwestern Mediterranean). Chlorophyll-*a* concentrations vary between 0.03 and 2.75 mg/m^3, though low values (<0.1 mg/m^3) are definitely more numerous ($\approx 70\%$). Most of them were sampled during the stratified season at sites exhibiting one, or seldom two, deep chlorophyll maxima (DCM) located in the 55–85-m depth interval.

2.3. Optical measurements

We also conducted optical measurements at selected sites during each cruise, totally 45 stations (see Fig. 1b). In-water downwelling irradiance (E_d) and upwelling radiance (L_u) profiles were taken in 32 stations using a Satlantic SPMR (SeaWiFS Profiling Multichannel Radiometer) that operates in 13 channels of the visible range (400, 412, 443, 470, 490, 510, 532, 555, 590, 620, 665, 683, and 700 nm). The data were acquired following the standard SeaWiFS protocols (Mueller & Austin, 1995). The instrument had been calibrated at Satlantic just before each cruise. The above-water measurements were made in the remaining 13 stations (when SPMR were not available) using the SIMBAD radiometer operating at 443, 490, 560, 670, and 870 nm. SIMBAD data were then processed at LOA (Laboratoire d'Optique Atmospherique) of the University of Lille (Fougnie, Deschamps, Frouin, & Mitchell, 1998). All optical measurements are hereafter used to derive the remote sensing reflectance (R_{rs}) and water leaving radiance (L_w) for algorithm validation.

Spectral in-water measurements of E_d and L_u have been propagated up to the surface ($z0^-$ level) using attenuation coefficients K_d and K_u, as estimated from the profiles. The corresponding above-water E_d and L_u ($z0^+$ level) were calculated according to the following equations:

$$L_u(0^+) = 0.54 L_u(0^-)$$

$$E_d(0^+) = 1/0.96 E_d(0^-)$$

where 0.54 is a mean coefficient summarizing the effect of internal reflection of the upwelling flux during transmission through the interface and 0.96 accounts for the loss of downwelling flux by reflection at the air–sea interface (Austin, 1974; Gordon et al., 1988; Morel & Antoine, 1994; O'Reilly et al., 1998). Both coefficients assume low solar zenith angle and calm sea surface, which were the experimental conditions of our measurements.

Finally, we computed R_{rs} at each wavelength λ, defined as $R_{rs}(\lambda)=L_u(0^+,\lambda)/E_d(0^+,\lambda)$ and $L_w(\lambda)$ multiplying R_{rs} by the mean extraterrestrial solar irradiance (Neckel & Labs, 1984) weighted by the spectral response of the relevant sensor bands, as proposed by O'Reilly et al. (1998).

2.4. SeaWiFS satellite data processing

High-resolution picture transmission (HRPT) SeaWiFS data have been acquired by the receiving station HROM at the Istituto di Fisica dell'Atmosfera (IFA), Rome, Italy, and transformed in Level 1A (L1A) standard NASA format. All the SeaWiFS passages relative to the period of in situ measurements were extracted from the IFA archive and processed up to Level 2 (L2) standard NASA format to obtain normalized water leaving radiance (L_{wn}) and remote sensing reflectance (R_{rs}) maps for the five available visible bands (412, 443, 490, 510, and 555 nm) using the SeaDAS software v.4.0B (Baith, Lindsay, Fu, & McClain, 2001). Siegel's atmospheric correction algorithm has been applied to L1A raw data (Siegel, Wang, Maritorena, & Robinson, 2000), which need a first estimate of chlorophyll-*a* concentration to compute water leaving radiances. Consequently, the L1A SeaWiFS data set was processed up to L2 for each selected algorithm (see Section 3). We opportunely modified the SeaDAS code to allow the application of the tested bio-optical algorithms, which are not present in the used SeaDAS software version.

Data have been remapped on a 1-km resolution equirectangular projection in the regions of interest, using the University of Miami Display Software Package (DSP). Final maps have been flagged by applying all of the 24 masks provided by SeaDAS (Baith et al., 2001). This implies that Saharan dust events have been implicitly excluded by our analysis.

3. Results

3.1. Algorithm presentation

To evaluate the performance of some representative empirical algorithms, we selected OC2v4 and OC4v4 (O'Reilly et al., 1998, 2000) as the NASA–SeaWiFS operational algorithms and the regional algorithm proposed by Gitelson et al. (1996) (hereafter GIT) as an example of a local Mediterranean algorithm. The functional forms of these algorithms are:

$$C = 10^{(a_0+a_1R+a_2R^2+a_3R^3)} + a_4 \quad (3.1)$$

for the OC2v4,

$$C = 10^{(a_0+a_1R+a_2R^2+a_3R^3+a_4R^4)} \quad (3.2)$$

for the OC4v4, and

$$C = a_0(10^R)^{a_1} \quad (3.3)$$

for GIT.

In Eq. (3.1), R is the $\log_{10}$ of the ratio between remote sensing reflectances, R_{rs}, measured at 490 and 555 nm. For the OC4v4 (Eq. (3.2)), R is the $\log_{10}$ of ratio of R_{rs} measured at 443 and 555, 490 and 555 nm, or 510 and 555 nm, depending on its value (the maximum is chosen). In the case of GIT, R is the $\log_{10}$ of ratio of the water leaving radiance, L_w, at 440 and 550 nm, and C is the total pigment concentration (chlorophyll-*a* + phaeopigments). The numerical value of the coefficients can be found in Table 1.

Table 1
Algorithm coefficients of OC2v4 (O'Reilly et al., 1998), OC4v4 (O'Reilly et al., 2000), and GIT (Gitelson et al., 1996) used in Eqs. (3.1), (3.2), and (3.3)

Algorithm	a_0	a_1	a_2	a_3	a_4	R
OC2v4	0.319	− 2.336	0.879	− 0.135	− 0.071	$\log_{10}(R_{rs}(490)/R_{rs}(555))$
OC4v4	0.366	− 3.067	1.930	0.649	− 1.532	$\log_{10}((R_{rs}443>R_{rs}(490)>R_{rs}(510))/R_{rs}(555)))$
GIT	0.914	− 1.86				$\log_{10}(L_{wn}(440)/L_{wn}(550))$

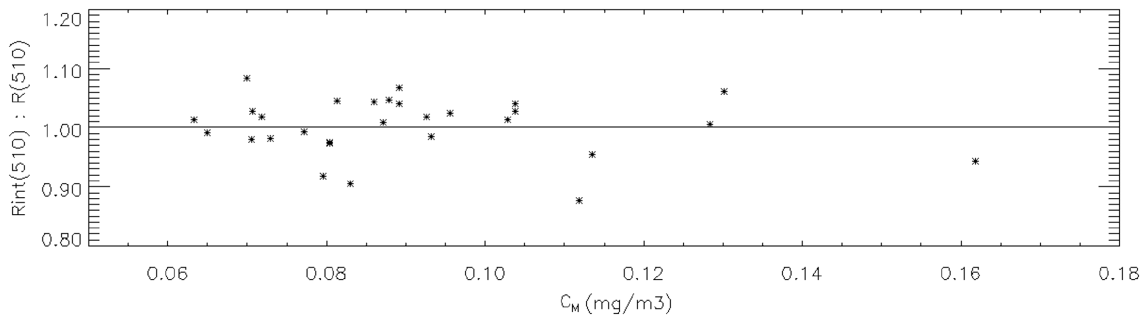

Fig. 2. The ratio of R_{rs} at 510 nm based on interpolated R_{rs} (R_{int}) to measured R_{rs} (R) versus chlorophyll-*a* concentration (C_M).

3.2. Algorithm validation

To test the performance of different algorithms in retrieving chlorophyll-*a* concentrations independently from atmospheric correction errors, we used only situ optical measurements (R_{rs}) and concurrent in situ chlorophyll-*a* data. Bio-optical estimates of chlorophyll-*a* (C_{mod}) were obtained by introducing the in situ R_{rs} measurements in the three selected algorithms presented in the previous section. For algorithms requiring data at wavelengths different from those available from in situ optical measurements (i.e., GIT and OC4v4 when applied to SIMBAD data), R_{rs} estimates have been generated using the interpolation procedure suggested by O'Reilly et al. (2000). The reliability of the interpolation procedure has been also verified by selecting R_{rs} values at 4 of the 13 bands available from SPMR measurements and then computing the remaining 9 R_{rs} via interpolation. The comparison between R_{rs}'s obtained by interpolation and those measured by SPMR is quite good and the error introduced by the interpolation appears to be less than 10%. Fig. 2 shows as an example the results obtained for the 510-nm band.

The validation procedure requires a comparison of algorithm chlorophyll-*a* estimates with concurrent in situ chlor-

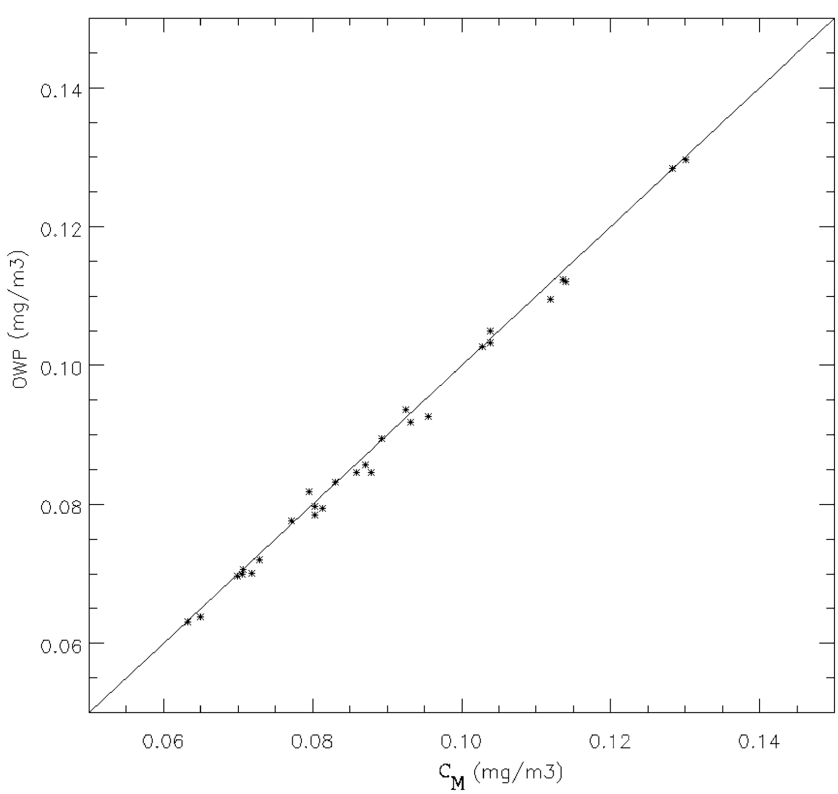

Fig. 3. Scatter plot of optical weighted pigment (OWP) concentration versus C_M. OWP is computed applying formula (6) in Clark (1997) to the chlorophyll-*a* profiles and using as $K_d(\lambda,z)$ as the measure obtained by concurrent SPMR Satlantic profiles at 490 nm. C_M is computed using Eq. (3.4) (see text).

ophyll-*a* concentrations (C_M). Following Gordon and Clark (1980), we computed C_M as:

$$C_M = \frac{\int_0^{Z_{pd}} C(z)\exp(-2kz)dz}{\int_0^{Z_{pd}} \exp(-2kz)dz} \quad (3.4)$$

where k is the attenuation coefficient for the downwelling PAR irradiance, $Z_{pd} = 1/k$ is the penetration depth and $C(z)$ can be either the chlorophyll-*a* or total pigment profile. Z_{pd} has been estimated as $Z_{pd} = Z_e/4.6$, with Z_e being the euphotic depth or the depth where PAR irradiance is reduced at 1% of its surface value. Z_e, in turn, has been determined for each station by the recursive method proposed by Morel and Berthon (1989) using calibrated fluorescence profiles as input. C_M refers to either C or $C+P$, according to the algorithm used.

C_M is very similar to the optically weighted pigment (OWP) concentration that "should be an accurate representation of the pigment concentration measured by a remote sensor viewing a stratified ocean" as reported by Clark (1997). The difference resides in the way of computing it and, in particular, in the definition of the lower limit for the integral computation. Clark's approach is based on the knowledge of diffuse attenuation coefficients of downwelling irradiance at various wavelengths ($K_{d,\lambda}$), while the C_M requires the knowledge of Z_e.

The presence of only above-water bio-optical measurements in some of the data set stations prevents the applica-

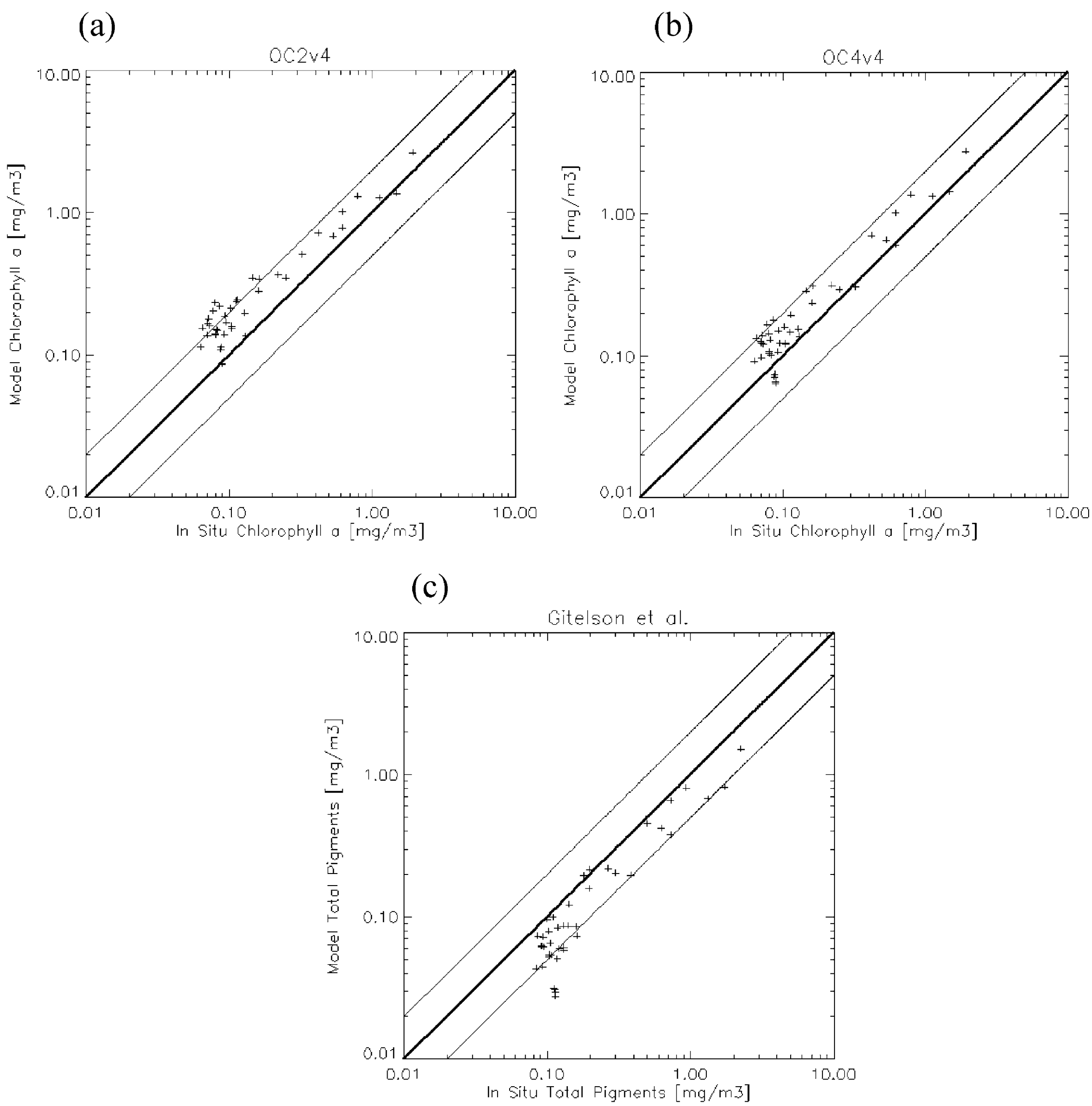

Fig. 4. Algorithm validation using in situ bio-optical measurements and concurrent in situ chlorophyll-*a* data C_M: (a) scatter plot of OC2v4 model values versus C_M; (b) scatter plot OC4v4 model values versus C_M; (c) scatter plot of GIT model values versus C_M. The 1:1 (center thick line), 1:2 (bottom thin line), and the 2:1 (top thin line) lines are also plotted.

Table 2
Application of the algorithm presented in Section 3.1 to the bio-optical in situ measurements versus in situ chlorophyll-*a* measurements (C_M): statistical analysis

Algorithm	$\%E_{min}$	$\langle\%E\rangle$	$\%E_{max}$	$\%S$	r^2
OC2v4	− 192	− 73	8	49	.945
OC4v4	− 128	− 40	28	41	.944
GIT	− 9	39	76	22	.930

The $\%E$ is obtained using Eq. (3.5). $\%E_{min}$, $\%E_{max}$, and $\langle\%E\rangle$ are the $\%E$ minimum, maximum, and average of $\%E$, respectively. $\%S$ is the standard deviation of $\%E$. r^2 is the correlation coefficient.

tion of Clark's approach to the entire bio-optical data set. When optical in-water profiles were available (i.e., $K_{d,\lambda}$'s were available), we performed a comparison between the two approaches, which confirmed the validity of using C_M instead of OWP (Fig. 3).

The C_M chlorophyll-*a* concentration collected in stations where bio-optical data are available ranges from 0.063 to 1.92 mg/m^3, covering the wide range of conditions of Case 1 waters of the Mediterranean Sea. Even if the number of stations is not very large, the bio-optical data set can be used to give indication of algorithm performances for most of the optical/biochemical provinces of the basin.

The results of the validation of the chlorophyll-*a* estimates by the three selected algorithms are shown in Fig. 4. The scatter plots clearly show that both NASA algorithms overestimate in situ chlorophyll-*a* measurements, while GIT

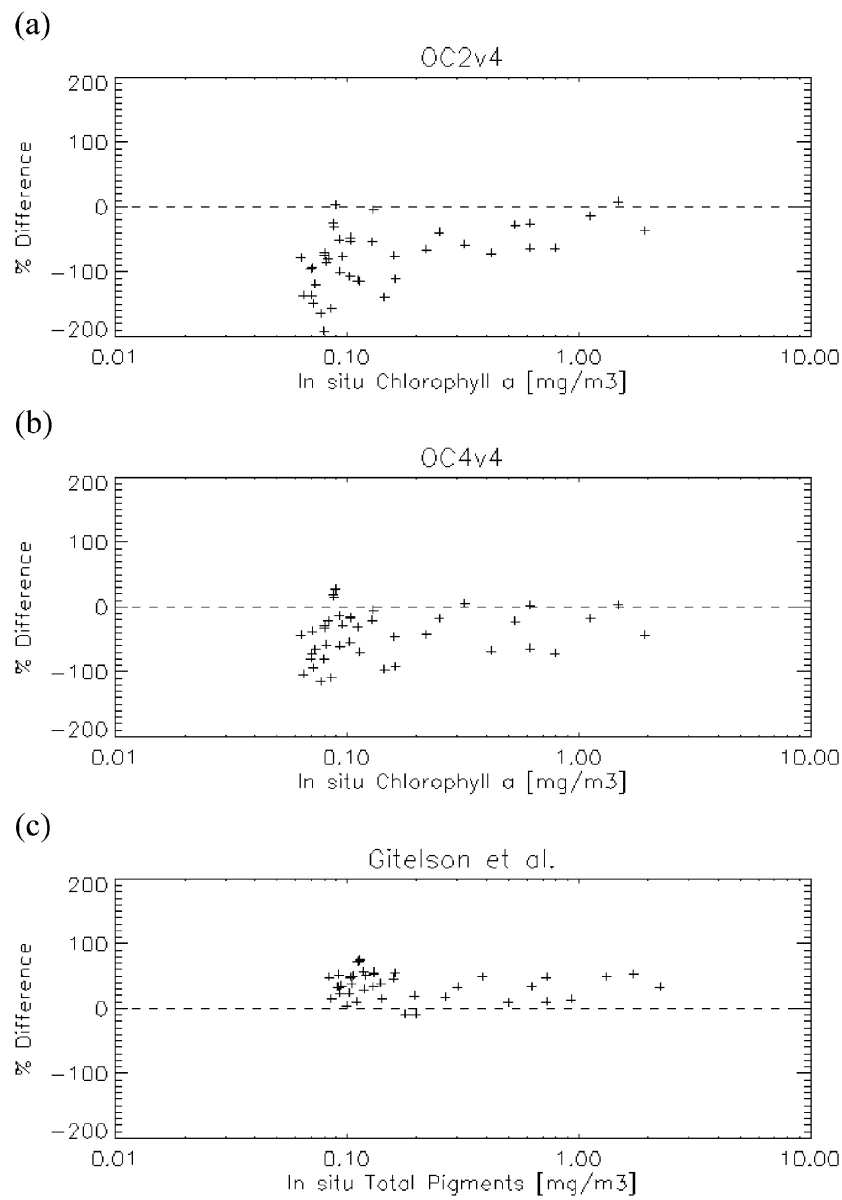

Fig. 5. Percentage differences between in situ chlorophyll-*a* data C_M and model values applied to bio-optical measurements in function of C_M: (a) C_M—OC2v4 versus C_M; (b) C_M—OC2v4 versus C_M;(c) C_M—GIT versus C_M.

algorithm underestimates C_M. To quantify errors, statistical parameters are summarized in Table 2 where percent error is defined as:

$$\%E = 100\left[\frac{C_M - C_{mod}}{C_M}\right] \tag{3.5}$$

with C_{mod} and C_M being the modelled and measured chlorophyll-*a*, respectively.

The squared correlation coefficient (r^2) of the modelled versus the in situ chlorophyll-*a* is nearly identical for OC4v4 (.944) and OC2v4 (.945), while GIT exhibits slightly lower r^2 (.930). Both OC2v4 and OC4v4 overestimate in situ observations by 73% and 40%, respectively. On the other hand, the GIT algorithm underestimates in situ observations by 39%. We also calculated the maximum and minimum percent deviation of the data from the model's estimates ($\%E_{min}$ and $\%E_{max}$ in Table 2), as well as the standard deviation of the percent error (%S in Table 2). The $\%E_{max}-\%E_{min}$ range and %S give an idea of the spreading of the data around the expected value (modelled chlorophyll-*a*). The %S values for the three algorithms range from 22% to 49% (Table 2). Moreover, it is noteworthy that in the case of NASA standard algorithms (more evidently for OC2v4), %E exhibits a correlation with C_M. Fig. 5 shows that the %E increases for low chlorophyll-*a* values with larger error at C_M lower than 0.15 mg/m^3 for both OC4v4 and OC2v4. On the contrary, the GITs %E is quite constant in the whole range of sampled C_M (Fig. 5c).

Even if the application of OC4v4 improves the OC2v4 chlorophyll-*a* estimates in the Mediterranean Sea, the results are still very poor. The GIT algorithm exhibits the best statistical performance between the three tested algorithms. However, the adoption of this algorithm as the standard Mediterranean regional algorithm is limited by three basic considerations. First, the 39% mean error we found is still greater than the 35% required by NASA. Second, the 440- and 550-nm bands used by GIT are no longer available in SeaWiFS or in the next generation ocean color sensors (e.g., MODIS MERIS). Last, the limited range of temporal and spatial coverage of the optical measurements used to develop the GIT algorithm ("21 locations were sampled on 22nd July 1992, in the southeastern Mediterranean," Gitelson et al., 1996) might prevent the applicability of this algorithm when applied to a different season or sea region.

Table 3
Statistical results of the new Mediterranean algorithm presented in Section 3.3 to the bio-optical in situ measurements versus in situ chlorophyll-*a* measurements (C_M)

Algorithm	$\%E_{min}$	$\langle\%E\rangle$	$\%E_{max}$	%S	r^2
L-DORMA	− 64	0.8	49	27	.948
NL-DORMA	− 62	1.8	52	27	.941

The %E is obtained using Eq. (3.5). $\%E_{min}$, $\%E_{max}$, and $\langle\%E\rangle$ are the %E minimum, maximum, and average of %E, respectively. %S is the standard deviation of %E. r^2 is the correlation coefficient.

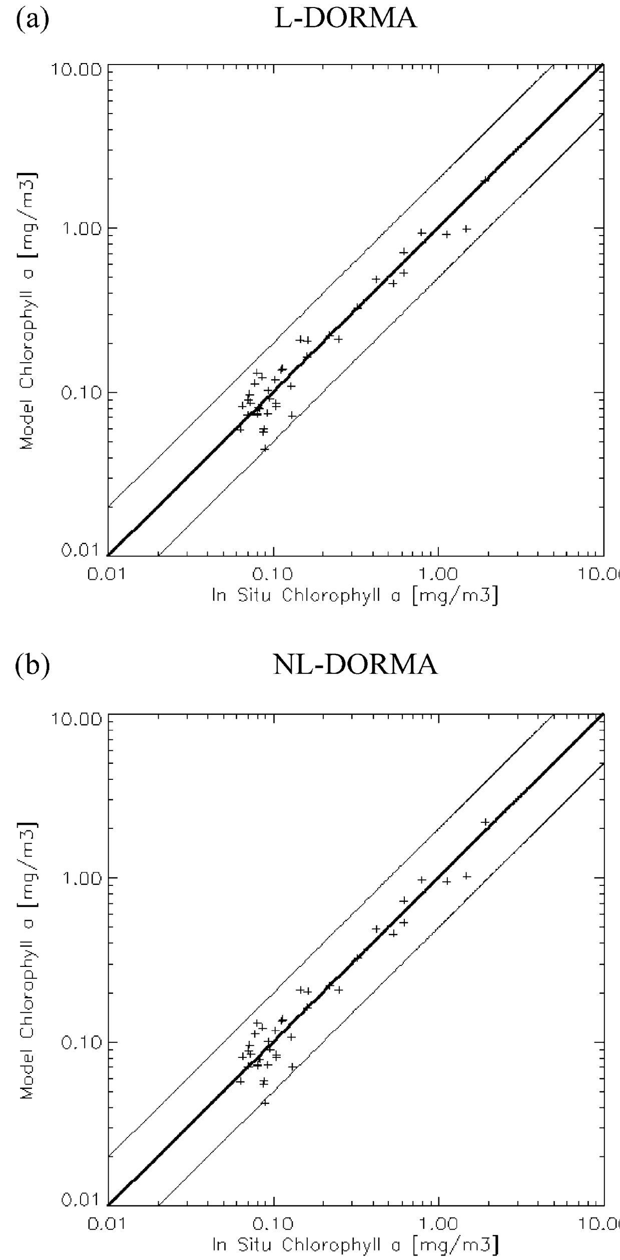

Fig. 6. Algorithm validation of the present paper algorithms using in situ bio-optical measurements and concurrent in situ chlorophyll-*a*: (a) scatter plot between L-DORMA model values versus C_M (b) scatter plot NL-DORMA versus concurrent in situ chlorophyll-*a* data C_M. The 1:1 (center thick line), 1:2 (bottom thin line), and the 2:1 (top thin line) lines are also plotted.

3.3. Algorithm adaptation

The algorithm validation (Section 3.2) suggests that a regional algorithm is needed for the Mediterranean Sea. Even if the bio-optical data set presented above consists of a limited number of data (45 stations), they represent most of the Mediterranean conditions ranging from oligotrophic to moderately eutrophic regimes. It is then possible to use this data set to develop a preliminary version of a Mediterranean ocean color algorithm. The distribution of the chlorophyll-*a* data versus band ratio suggests that both linear and polynomial function can be used to develop an ad hoc algorithm.

The limited size of our data set suggests the use of a simpler algorithm than OC4v4. In fact, to compute new coefficients for an OC4-like algorithm we need that, after the selection criterion, all the three possible band ratios should be represented by a significant number of data points in the data set used. Moreover, the application of the OC4v4 selection band ratio criterion to our data set results in a net predominance of the R_{555}^{443} band ratio selection, while the R_{555}^{510} is practically never selected.

Thus, we derived two new sets of coefficients for both the linear and OC2 functional forms. The coefficients are derived from regressions using our 45 data points.

The new polynomial equation NL-DORMA (NonLinear-D'ORtenzio MArullo, Eq. (3.6)) is:

$$C = 10^{(0.217 - 2.728R + 0.704R^2 + 0.297R^3)} - 0.035 \qquad (3.6)$$

while the new linear equation L-DORMA (Linear-D'ORtenzio MArullo, Eq. (3.7)) is

$$C = 1.49 \times 10^{(-2.51R)} \qquad (3.7)$$

where $R = \log_{10}(R_{rs}(490)/R_{rs}(555))$.

In the polynomial fit case, the regression was constrained to reproduce OC2v4-derived values for high chlorophyll-*a* concentrations. The statistical results of the new regressions are summarized in Table 3.

It is evident that the application of linear or polynomial forms gives similar results once the coefficients are optimized with respect to the data. In Fig. 6, the comparison between the two new models and the in situ chlorophyll-*a* data shows that the points are now distributed around the line of best agreement with a percent error that rarely exceeds 35%.

3.4. Satellite match-up analysis

The algorithm validation presented in the previous sections, however, supplies only partial information about the performance of the algorithms when applied to satellite-derived water leaving radiances. For this reason, we performed a validation of the algorithms by comparing satellite estimates with concurrent in situ chlorophyll-*a* observations. The validation procedure was applied to the algorithm presented in Section 3.1, as well as to the algorithm developed in Section 3.3. Moreover, we considered also the Neural Network Algorithm (NNA) to complete the list of the algorithms provided by NASA's standard processing system (Gross, Thiria, Frouin, & Mitchell, 2000).

The chlorophyll-*a* profiles that match in time and space with concurrent satellite passages constitute the match-up data set (C_{situ}). Note that C_{situ} and C_M data sets only partially overlap, because C_M includes all those stations where chlorophyll-*a* profiles and optical measurements were present at the same time, while C_{situ} includes the stations where chlorophyll-*a* measurements match in time and location with a valid satellite pixel (match-up analysis). C_{situ}

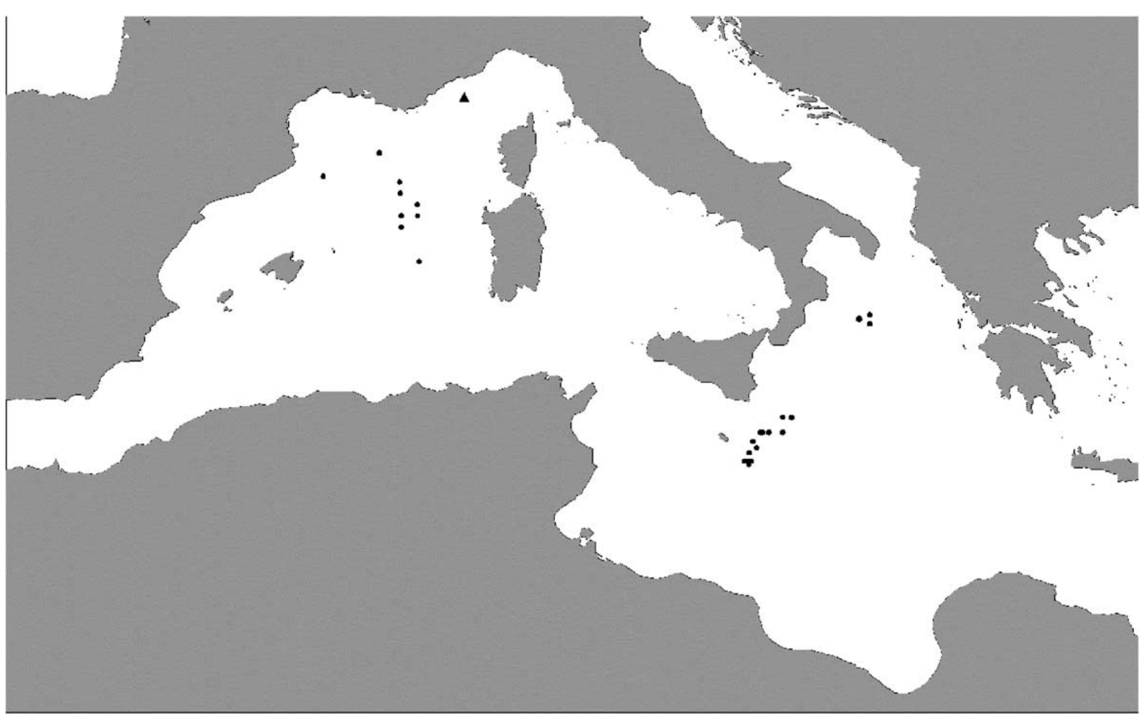

Fig. 7. Geographical distribution of the satellite and in situ chlorophyll-*a* match-up data.

Table 4
Application of the tested algorithm to satellite data versus in situ chlorophyll-*a* measurements (C_{situ}): statistical analysis

Algorithm	$\langle\%E_{sat}\rangle$	$\langle\%E^-_{sat}\rangle$	$\langle\%E^+_{sat}\rangle$	$\%S_{sat}$	$\%S^-_{sat}$	$\%S^+_{sat}$	r^2
OC2v4	− 84.9	− 96.2	− 9.8	69.4	66.9	25.0	.932
OC4v4	− 116.2	− 131.3	− 15.6	81.4	75.8	29.0	.928
NNA	− 143.6	− 162.3	− 18.8	93.0	84.3	32.3	.869.
GIT	9.7	5.1	40.3	40.4	41.0	16.5	.932
NL-DORMA	− 28.1	− 31.7	− 4.3	50.0	51.9	26.4	.916
L-DORMA	− 9.5	− 14.7	25.2	37.0	36.2	20.6	.927

The $\%E_{sat}$ is obtained using Eq. (3.8). $\langle\%E_{sat}\rangle$ and $\%S_{sat}$ are the average and the standard deviation of $\%E_{sat}$, respectively. $\langle\%E^-_{sat}\rangle$ and $\%S^-_{sat}$ are the average and the standard deviation of $\%E_{sat}$ for values of $C_{situ} < 0.15$ mg/m^3, respectively. $\langle\%E^+_{sat}\rangle$ and $\%S^+_{sat}$ are the average and the standard deviation of $\%E_{sat}$ for values of $C_{situ} > 0.15$ mg/m^3, respectively. r^2 is the correlation coefficient.

has been calculated using the same formulation (Eq. (3.4)) used for C_M.

The match-up file has been produced using a time window of 8 h centered on the satellite pass time. Each satellite-derived parameter has been averaged on 3 × 3 pixels centered at the location of each station where chlorophyll-*a* profiles were available, using only those pixels that passed all the above-cited exclusion criteria (see Section 2.4). A threshold of eight valid pixels was set to include the data points in the match-up file.

After the selection procedure outlined above, we were able to sort out 46 match-up points (including the six points acquired by the DYFAMED, station) for our analysis (the location of the match-up points is shown in Fig. 7). These data cover a range of C_{situ} values from 0.05 to 1.14 mg/m^3 of chlorophyll-*a* concentration (0.06–1.34 mg/m^3 of pigment concentration) with a significant prevalence of values typical of the Mediterranean oligotrophic regime ($C_{situ} < 0.1$ mg/m^3). All the data exceeding 1 mg/m^3 (7 %) have been collected in the northwest Mediterranean, during the intense bloom occurring at the end of winter 2000. This area is among the few where the Mediterranean Sea does not display its characteristic oligotrophic regime. It is noteworthy that the number of locations where C_{situ} and C_M overlap is only five. In these five stations, optical measurements, chlorophyll-*a* profiles, and satellite estimates are present at the same time.

The results of the match-up analysis for the different algorithms are summarized in Tables 4 and 5 and in Fig. 8, essentially confirming the picture revealed by the analysis of the in situ bio-optical data (see Fig. 4). In brief, the standard NASA algorithms (OC2v2, OC4v4, and NNA) overestimate C_{situ}, while the algorithms tuned over the Mediterranean Sea (GIT, NL-DORMA, and L-DORMA) are definitively closer to the in situ data. Table 4 contains information about the percent error ($\%E_{sat}$) defined as:

$$\%E_{sat} = 100\left[\frac{C_{situ} - C_{sat}}{C_{situ}}\right] \tag{3.8}$$

where C_{sat} is the satellite estimate. The standard deviation of the percent error for the whole data set ($\%S_{sat}$) is also reported. In addition, the same parameters have been estimated separately for low ($\%E^-_{sat}$) and high ($\%E^+_{sat}$) C_{situ} concentrations ($C_{situ} < 0.15$ and $C_{situ} > 0.15$ mg/m^3) to evidence the performance of selected algorithms in the oligotrophic regime predominant in most Mediterranean basins.

The high values of the mean $\%E_{sat}$ ($\langle\%E_{sat}\rangle$) for the three global scale algorithms is essentially due to the strong overestimation in the low chlorophyll-*a* range. Nevertheless, the performances in the high chlorophyll-*a* range are still acceptable. Contrary to what was observed in the analysis of the in situ bio-optical data, the OC2v4 chlorophyll-*a* estimates agree better than the other two global algorithms when applied to the satellite data. The NNA estimates are definitely the worst.

The Mediterranean algorithms generally exhibit better results: the $\langle\%E_{sat}\rangle$ is definitively within 35% value defined as one of the requirements of the SeaWiFS project (Hooker & McClain, 2000). More in details, the Mediterranean linear algorithms (GIT and L-DORMA) show a mean $\%E^-_{sat}$ ($\langle\%E^-_{sat}\rangle$) lower than the mean $\%E^+_{sat}$ ($\langle\%E^+_{sat}\rangle$), signifying that a better estimate occurs in the low chlorophyll-*a* range. The GIT algorithm, in particular, exhibits an unacceptable $\langle\%E^+_{sat}\rangle$ of 40.3%. On the other hand, the mean values of the absolute error ($\Delta C = C_{situ} - C_{sat}$) (Table 5), relative to the two DORMA algorithms, are very close in the low C_{situ} range, but are definitively better for the NL-DORMA in the high C_{situ} region (see Table 5, under

Table 5
Application of the tested algorithm to satellite data versus in situ chlorophyll-*a* measurements (C_{situ}): statistical analysis

Algorithm	$\langle\Delta C\rangle$ (mg/m^3)	$\langle\Delta C^-\rangle$ (mg/m^3)	$\langle\Delta C^+\rangle$ (mg/m^3)	S (mg/m^3)	S^- (mg/m^3)	S^+ (mg/m^3)	r^2
OC2v4	− 0.074	− 0.077	− 0.054	0.071	0.044	0.172	.932
OC4v4	− 0.101	− 0.105	− 0.081	0.072	0.041	0.183	.928
NNA	− 0.134	− 0.133	− 0.143	0.110	0.058	0.287	.869
GIT	0.053	0.012	0.326	0.128	0.037	0.183	.932
NL-DORMA	− 0.021	− 0.021	− 0.019	0.080	0.041	0.212	.916
L-DORMA	0.025	− 0.006	0.233	0.107	0.033	0.185	.927

The ΔC is defined as: $\Delta C = C_{situ} - C_{sat}$. $\langle\Delta C\rangle$ and S are the arithmetic mean and the standard deviation of ΔC, respectively. $\langle\Delta C^-\rangle$ and S^- are the arithmetic mean and the standard deviation of ΔC for value of $C_{situ} < 0.15$ mg/m^3. $\langle\Delta C^+\rangle$ and S^+ are the arithmetic mean and standard deviation of ΔC for value of $C_{situ} > 0.15$ mg/m^3, respectively. r^2 is the correlation coefficient.

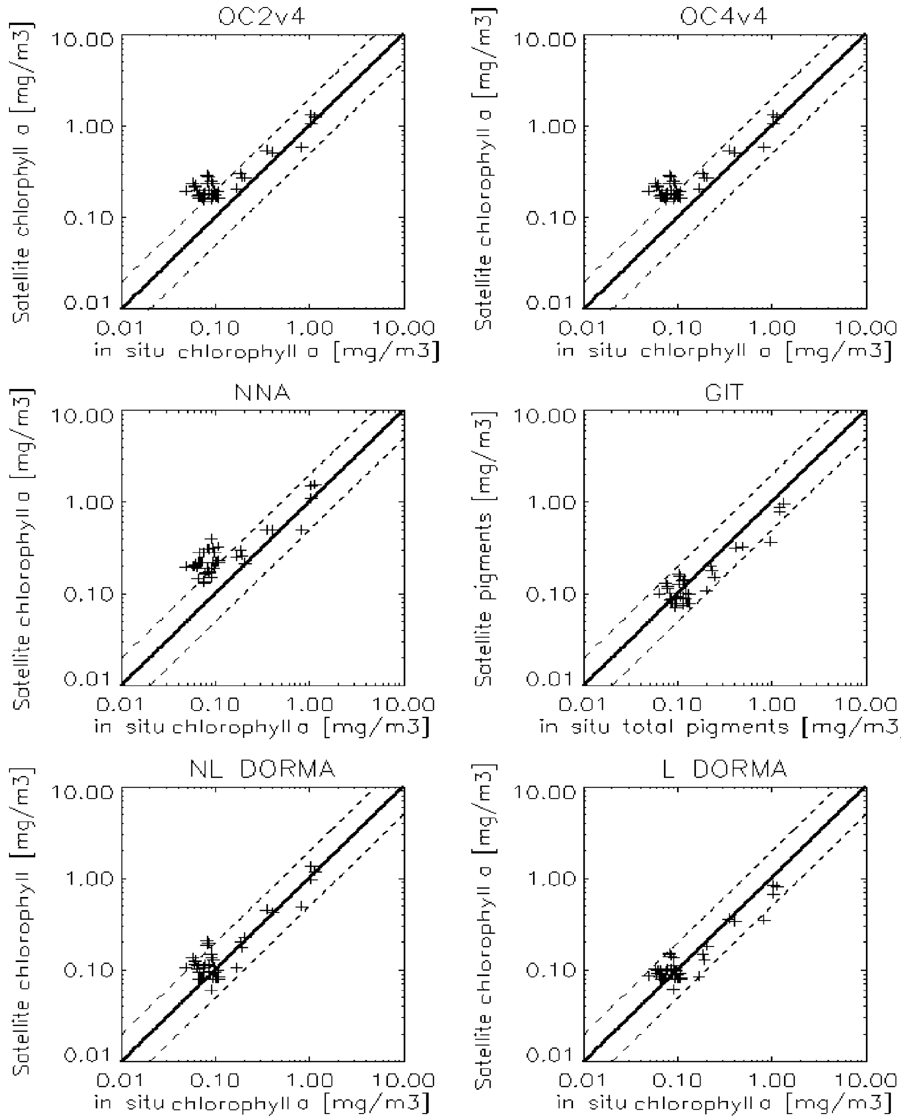

Fig. 8. SeaWiFS chlorophyll-*a* estimates (C_{sat}) validation against concurrent in situ chlorophyll-*a* data C_{situ}: (a) scatter plot of SeaWiFS estimate using OC2v4 model values versus C_M; (b) scatter plot of SeaWiFS estimate using OC4v4 model values versus C_M; (c) scatter plot of SeaWiFS estimate using Neural Network model values versus C_M; (d) scatter plot of SeaWiFS estimate using GIT model values versus C_M; (e) scatter plot of SeaWiFS estimate using NL-DORMA model values versus C_M. (f) scatter plot of SeaWiFS estimate using L-DORMA model values versus C_M. The 1:1 (center thick line), 1:2 (bottom thin line), and the 2:1 (top thin line) lines are also plotted.

$\langle \Delta C^+ \rangle$). The difference in the sign of $\langle \Delta C \rangle$ and $\langle \%E_{sat} \rangle$ for the L-DORMA algorithm (Tables 4 and 5) is due to the different relative weight of the errors in the chlorophyll estimates. The negative sign of the $\langle \%E_{sat} \rangle$ demonstrates that most of the percent error is due to the general underestimation of the algorithm, while the positive sign of $\langle \Delta C \rangle$ account for a higher weight of the overestimated values on the mean error.

4. Discussion

All the results presented in the previous section raise the question of why the global algorithms overestimate chlorophyll-*a* concentration in the Mediterranean Sea.

A possible cause, which could bias the satellite reflectance ratio as compared to the one expected from in situ pigment concentrations, was discussed by Gitelson et al. (1996). They proposed that a relatively higher abundance of coccolithophores as compared to other groups, which might be typical of oligotrophic open seas, would in fact distort the reflectance ratios. It is noteworthy that this argument holds for relatively low concentrations of coccolithophores, well below the concentrations that make the global algorithms unfit and that are flagged by the routine procedure. This point is quite intriguing, because it is generally assumed that coccolithophore chlorophyll-*a* should be underestimated owing of the peculiar calcareous coverage of the cells (Gordon and Balch, 1999), with an enhanced reflectance in the visible part of the spectrum (Tyrrell, Holligan, & Mobley, 1999).

The effect of the coccolithophores presence on the blue-green water leaving radiance ratio had already been described by Gordon and Balch (1999). They underlined the change in the behavior of the $L_{wn}(440)/L_{wn}(550)$ ratio when coccolith concentration ranges between 0 and 200×10^9 coccoliths/m^3.

Then, to figure out whether the Gitelson hypothesis holds, we performed an analysis similar to that by Gordon and Balch (1999), but applied to the band ratio used in the NL-DORMA and OC2 (i.e., 490/555 nm). We modelled the R_{rs} using the Gordon et al. (1988) assumption (Eq. (4.1)):

$$R_{rs}(\lambda) = 0.095\left(\frac{b_b(\lambda)}{b_b(\lambda) + a(\lambda)}\right)0.54 \tag{4.1}$$

where b_b is the total backscattering coefficient and a is the total absorption coefficient.

Absorption coefficient has been calculated according to the bio-optical model of Morel (1991) for Case 1 waters (Eq. (4.2)):

$$a = a_w + a_p + a_{CDOM} \tag{4.2}$$

where the subscripts w, p, and CDOM refer to seawater, particulate, and colored dissolved organic matter contributions to the total absorption coefficient, respectively. $a_w(\lambda)$ has been estimated according to Smith and Baker (1978), a_{CDOM} has been estimated assuming that CDOM concentration covaries with chlorophyll-*a*, and with a spectral dependence described by an exponential function with an exponent of -0.014 (Bricaud, Morel, & Prieur, 1981). a_p has been modelled following Morel (1991) using chlorophyll-*a* specific absorption coefficients proposed by Sathyendranath and Platt (1988).

Following Tyrrell et al. (1999), we expressed b_b as (Eq. (4.3)):

$$b_b = b_{bw} + b_{bp} + b_{b,CaCO_3} \tag{4.3}$$

where b_{bw} is the backscattering coefficient of seawater, computed as Morel's (1974), b_{bp} is the backscattering coefficient of particulate, and $b_{b,CaCO_3}$ is the backscattering coefficient due to the calcite ($CaCO_3$) of coccoliths (for details, see Eqs. (5), (6), and (8) in Tyrrell et al., 1999). We used the values of the optical properties, composition, and abundance of coccoliths given by Tyrrell et al. (1999) and we also assumed that the coccoliths covering the cells have the same optical properties of the detached ones. Simulations showed a decrease in reflectance ratio as calcite concentrations increased, confirming the results obtained by Gordon and Balch (1999) for CZCS bands, providing a cue for the overestimation of chlorophyll-*a* at low levels.

However, the derived reflectance ratio fits our experimental bio-optical data (Fig. 9) for a $CaCO_3$ concentration of about 5 mg/m^3. This amount of calcite would in fact correspond to a coccolithophore concentration between 3×10^4 and 2.5×10^5 cells/dm^3, which is almost one order of magnitude higher than the concentration found by the SZN group (4000 cells/dm^3) in few stations of the Ionian Sea (Rabitti, Civitarese, & Ribera d'Alcalà, 1994) or reported by Robarts, Zohary, Waiser, and Ycobi (1996) and Yacobi et al. (1995) in the Levantine Sea.

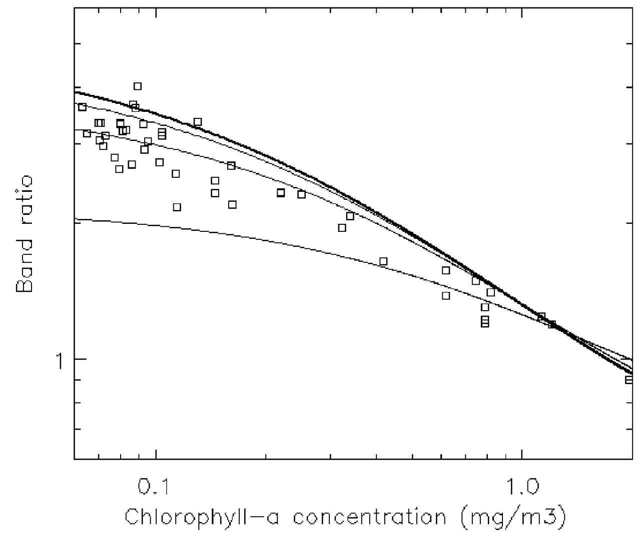

Fig. 9. Variations in the $R_{rs}(490)/R_{rs}(555)$ band ratio with chlorophyll-*a* concentration. Squares represent the in situ bio-optical measurements and the concurrent chlorophyll-*a* presented in Section 2.3. The solid line is the semi-analytic radiance model presented in Section 4. The $CaCO_3$ concentrations for the four lines are 0, 1, 5, and 50 mg/m^3. The thick line represents the lower $CaCO_3$ concentration. The higher $CaCO_3$ concentrations yield the "flatter" curves.

Thus, the observed systematic overestimate can only partially be explained by the presence of coccolithophores.

A distortion in the reflectance ratio could also originate from a high concentration of CDOM, which might be higher in the Mediterranean Sea, a semi-enclosed basin, than in the open ocean. We do not have CDOM concurrent data with chlorophyll-*a* data, but measurements recently carried out in open waters of Mediterranean Sea display very low concentrations of CDOM, always between 50 and 80 μmol/dm^3 (Seritti et al., 2000).

Therefore, the lower value of the measured band ratio is probably due to a phytoplankton community with optical properties different from the average community on which OC2v4 is based, similarly to what Sathyendranath, Cota, Stuart, Maass, and Platt (2001) observed for the Labrador Sea. This, in turn, stresses even more the need for regional algorithms.

Furthermore, because satellite-derived geophysical quantities, such as chlorophyll-*a*, are retrieved from measurements taken above the atmosphere we also tried to quantify the possible error induced by the atmospheric correction term.

The different behavior of the same algorithm when applied to bio-optical measurements or to remotely sensed data demonstrates that the atmospheric correction is still the main source of error in ocean color data. In addition, the use of the atmospheric correction Siegel algorithm increases the dependency between the atmospheric correction procedure and the preliminary estimate of chlorophyll-*a* and consequently between the atmospheric correction and the used bio-optical algorithm.

In general, the application of the algorithms to the satellite data led to an increase in the satellite-derived chlorophyll-*a* estimates. This effect is particularly evident for OC4v4, which is probably more affected by the error in the atmospheric correction, because of the multiple band ratio option. The poor performance of this algorithm in the satellite chlorophyll-*a* retrieval is evident from our analysis, even if it exhibits better results than OC2v4 when applied to in situ bio-optical data.

We mentioned before that we intentionally took out from our analysis the observations with problematic aerosol conditions, e.g., Saharan dust. Therefore, the optical properties exhibited by the Mediterranean atmosphere could depend on aerosol load and composition (see Liberti et al., 2001), which in turn could be related to the close connection of the sea with the land.

5. Conclusions

The major aim of this paper is the validation of some representative empirical algorithms to determine their performance in retrieving chlorophyll-*a* concentration in the Mediterranean Sea from SeaWiFS data. We selected three algorithms: OC2v4 and OC4v4, as NASA's operational algorithms, and GIT (Gitelson et al., 1996), as an example of a regional Mediterranean algorithm.

As anticipated in the Introduction, discrepancies, if any, between SeaWiFS standard algorithms and Mediterranean applications could rise either from failures in atmospheric correction procedures or from peculiar bio-optical characteristics of the Mediterranean waters. To avoid the problem arising from the atmospheric correction procedure, a data set of bio-optical measurements has been collected in the Mediterranean Sea.

The analysis of bio-optical measurements revealed a systematic overestimation of chlorophyll-*a* concentration by NASA global algorithms. The error appears to be correlated with chlorophyll-*a* concentration, by exhibiting marked differences at low values ($C < 0.15$ mg/m^3). In particular at low concentration, the bias observed for OC2v4 is about twice that observed for OC4v4.

On the other hand, when the NASA standard algorithms are applied to remotely sensed data, the behavior appears reversed: the OC2v4 algorithm exhibits better estimates than OC4v4, which is probably more affected by atmospheric correction problems.

Thus, on the basis of our data, we are not able to define which NASA standard algorithm should be preferred for the Mediterranean region.

On the other hand, the regional algorithm proposed by Gitelson et al. (1996) for the southeastern Mediterranean Sea overestimates the measured total pigment concentration when applied to the bio-optical data. However, it does not exhibit a correlation between the error and the measures. When applied to satellite data, the GIT algorithm still performs better than the NASA global algorithms, although the estimates are very poor in the high chlorophyll-*a* range.

On the basis of these considerations, it appears evident that the GIT algorithm performs best. However, the GIT algorithm was tuned to retrieve total pigment concentration rather than chlorophyll-*a* concentration. Moreover, this algorithm uses the CZCS bands, some of which are not available on SeaWiFS.

It is evident that the algorithms selected in this paper were not able to give chlorophyll-*a* estimates for the Mediterranean Sea that satisfied NASA requirements (i.e., 35% error in chlorophyll-*a* concentration). For this reason, we introduce two new algorithms, retrieved by fitting our Mediterranean bio-optical data set with linear and OC2-like functional forms. The new algorithms perform well when applied either to the bio-optical measurements or to satellite data. Due to the relatively small number of available in situ data, the algorithms that we generated have to be considered very preliminary and it is not even certain that a future Mediterranean ocean color algorithm will be unique for the whole basin. Nevertheless, the restricted range of chlorophyll-*a* concentrations in Mediterranean Case 1 waters, which allowed to fit satisfactorily the data with a linear regression, and the extendibility of the Gitelson algorithm make us more confident that one single algorithm might work, at least for basic quantities, such as chlorophyll-*a* and derived properties.

A larger data set of bio-optical in situ measurements is obviously necessary. But, because of the above-discussed Mediterranean peculiarities, it is also necessary to build a data set of atmospheric parameters to allow a refinement of atmospheric correction algorithms.

SeaWiFS undoubtedly represents a dramatic improvement in the observation of marine ecosystems from the space, especially due to enhanced spatial and time coverage and the forthcoming new generation of optical sensors will further expand this capability.

We showed that a region like the Mediterranean Sea requires an independent treatment of the atmospheric and the in-water bio-optical term to obtain reliable estimates of phytoplankton activity. This might also allow to test and to better understand the contribution of different radiative transfer terms in real environments.

Alternative semi-empirical or totally empirical approaches, such as neural networks (Schiller & Doerffer, 1999), genetic algorithms (Robilliard, Chami, Fonlupt, & Santer, 2000), and inverse methods (Hoge, Wright, Lyon, Swift, & Yungel, 1999), would probably solve the problem of decreasing retrieval errors, though without shedding light of what are the determinant modulating factors that differentiate one region from another.

According to Antoine et al. (1995) and Morel and André (1991), more than 70% of primary production in the Mediterranean basin is due to the oligotrophic regions. Because the relative error in the lower range of chlorophyll-*a* concentration is much higher, an overestimation of pigment concentration would generate an error in the primary production retrieval. Therefore, a finely tuned algorithm is necessary for regional seas.

Acknowledgements

This work was supported by the Agenzia Spaziale Italiana (ASI) in the framework of the project "Uso integrato di dati da satellite ed in situ per lo studio della relazione tra dinamica a mesoscala e produttività nel Mar Mediterraneo" under the contracts ARS-00-21.

The authors would like to thank the Laboratoire d'Optique Atmospherique of the University of Lille for the SIMBAD data and the Service d'Observation DYFAMED (SODYF) for the DYFAMED data. The authors would also like to thank Dr. Francesco Bignami for his vigorous encouragement and stimulating discussion.

References

Abbott, M. R., & Chelton, D. B. (1991). Advances in passive remote sensing of the ocean. *Review of Geophysics*, 571–589.

Antoine, D., Morel, A., & André, J.-M. (1995). Algal pigment distribution and primary production in the eastern Mediterranean as derived from Coastal Zone Color Scanner observations. *Journal of Geophysical Research*, *100*, 16193–16209.

Austin, R. W. (1974). The remote sensing of spectral radiance from below the ocean surface. In N. G. Jerlov, & E. Steemann-Nielsen (Eds.), *Optical aspects of oceanography* (pp. 317–344). London: Academic Press.

Baith, K., Lindsay, R., Fu, G., & McClain, C. R. (2001). SeaDAS: data analysis system developed for ocean color satellite sensors. *Eos, Transactions of the American Geophysical Union*, *82*, 202–205.

Barale, V., & Schlittenhardt, P. M. (1993). *Ocean colour: theory and applications in a decade of CZCS experience*. Dordrecht: Kluwer Academic Publishers.

Barnes, W. L., Pagano, T. S., & Salomonson, V. V. (1998). Prelaunch characteristics of the Moderate Resolution Imaging Spectroradiometer (MODIS) on EOS-AM1. *IEEE Transactions on Geoscience and Remote Sensing*, *36*, 1088–1100.

Bricaud, A., Morel, A., & Prieur, L. (1981). Absorption by dissolved organic matter of the sea (yellow substance) in the UV and visible domains. *Limnology and Oceanography*, *26*, 43–53.

Carder, K. L., Chen, F. R., Lee, Z. P., Hawes, S. K., & Kamykowski, D. (1999). Semi-analytic MODIS algorithms for chlorophyll a and absorption with bio-optical domains based on nitrate-depletion temperatures. *Journal of Geophysical Research*, *104*, 5403–5421.

Clark, D. K. (1997). *Bio-optical algorithms—Case 1 waters.* MODIS algorithm theoretical basis document 19.

Dierssen, H. M., & Smith, R. C. (2000). Bio-optical properties and remote sensing ocean color algorithms for Antarctic Peninsula waters. *Journal of Geophysical Research*, *105*, 26301–26312.

Doerffer, R., Sorensen, K., & Aiken, J. (1999). MERIS potential for coastal zone applications. *International Journal of Remote Sensing*, *20*, 1809–1818.

ENVISAT Cal-Val Team (2000). *ENVISAT: calibration and validation plan.* ESA Technical Report. PO-PL-ESA-GS-1092.

Esaias, W. E., Abbott, M. R., Barton, I., Brown, O. B., Campbell, J. W., Carder, K. L., Clark, D. K., Evans, R. H., Hoge, F. E., Gordon, H. R., Balch, W. M., Letelier, R., & Minnett, P. J. (1998). An overview of MODIS capabilities for ocean science observations. *IEEE Transactions on Geoscience and Remote Sensing*, *36*, 1250–1265.

Fargion, G. S., & McClain, C. R. (2000). Three years of ocean color instrument intercomparisons and cross-calibrations by the SIMBIOS project (1997–2000). In C. R. Bostater, & R. Santoleri (Eds.), *Remote sensing of the ocean and sea ice 2000. Proceedings of the SPIE, vol. 4172* (pp. 44–55). Barcelona: NASA.

Fougnie, B., Deschamps, P. Y., Frouin, R., & Mitchell, B. G. (1998). Measuring water-leaving radiance with a polarization radiometer: theory and experimental verification. *EOS Transactions*, *79*(1), 99.

Gilman, C., & Garrett, C. (1994). Heat flux parameterizations for the Mediterranean Sea: the role of atmospheric aerosols and constraints from the water budget. *Journal of Geophysical Research*, *99*, 5119–5134.

Gitelson, A., Karnieli, A., Goldman, N., Yacobi, Y. Z., & Mayo, M. (1996). Chlorophyll estimation in the SE Mediterranean using CZCS images: adaptation of an algorithm and its validation. *Journal of Marine System*, *9*, 283–290.

Gordon, H. R., & Balch, W. M. (1999). *MODIS detached coccolith concentration.* MODIS algorithm theoretical basis document 19.

Gordon, H. R., Brown, O. B., Evans, R. H., Brown, J. W., Smith, R. C., Baker, K. S., & Clark, D. K. (1988). A semianalytic radiance model of ocean color. *Journal of Geophysical Research*, *93*, 10909–10924.

Gordon, H. R., & Clark, D. (1980). Remote sensing optical properties of a stratified ocean: an improved interpretation. *Applied Optics*, *19*, 3428–3430.

Gordon, H. R., & Morel, A. (1983). Remote assessment of ocean color for interpretation of satellite visible imagery. In R. T. Barber, N. K. Mooers, M. J. Bowman, & B. Zeitzschel (Eds.), *A review, lecture notes on coastal and estuarine studies* (pp. 1–114). New York: Springer-Verlag.

Gordon, H. R., & Wang, M. (1994). Retrieval of water-leaving radiance and aerosol optical thickness over the oceans with SeaWiFS: a preliminary algorithm. *Applied Optics*, *33*, 443–452.

Gregg, W. W., & Conkright, M. E. (2001). Global seasonal climatologies of ocean chlorophyll: blending in situ and satellite data for the CZCS era. *Journal of Geophysical Research*, *106*, 2499–2515.

Gross, L., Thiria, S., Frouin, R., & Mitchell, B. G. (2000). Artificial neural networks for modeling the transfer function between marine reflectance and phytoplankton pigment concentration. *Journal of Geophysical Research*, *105*, 3483–3495.

Guerzoni, S., Molinaroli, A., & Chester, W. (1997). Saharan dust inputs to the western Mediterranean Sea: depositional patterns, geochemistry and sedimentological implications. *Deep-Sea Research*, *44*, 631–640.

Harris, G. P., Feldman, G. C., & Griffiths, F. B. (1993). Global oceanic production and climate change. In V. Barale, & P. M. Schlittenhardt (Eds.), *Ocean colour: theory and applications in a decade of CZCS experience* (pp. 237–270). Dordrecht: Kluwer Academic Publishers.

Hoge, F. E., Wright, C. W., Lyon, P. E., Swift, R. N., & Yungel, J. K. (1999). Satellite retrieval of inherent optical properties by inversion of an oceanic radiance model: a preliminary algorithm. *Applied Optics*, *38*, 495–504.

Hooker, S. B., & McClain, C. R. (2000). The calibration and validation of SeaWiFS data. *Progress in Oceanography*, *45*, 427–465.

Hooker, S. B., McClain, C. R., & Holmes, A. (1993). Ocean color imaging: CZCS to SeaWiFS. *MTS Journal*, *27*, 3–15.

Jorgensen, P. V. (1999). Standard CZCS Case 1 algorithms in Danish coastal waters. *International Journal of Remote Sensing*, *20*, 1289–1301.

Kahru, M., & Mitchell, B. G. (1999). Empirical chlorophyll algorithm and preliminary SeaWiFS validation for the California Current. *International Journal of Remote Sensing*, *20*, 3423–3429.

Léon, J. F., Chazette, P., & Dulac, F. (1999). Retrieval and monitoring of aerosol optical thickness over an urban area by spaceborne and ground-based remote sensing. *Applied Optics*, *38*, 6918–6926.

Liberti, G. L., D'Ortenzio, F., Santoleri, R., McClain, C., Wang, M., & Volpe, G. (2001). *Validation of the SeaWiFS aerosol products over* *the Mediterranean Sea*. The EUMETSAT meteorological satellite data users' conference, 1–5 October 2001, Antalya, Turkey.

Marty, J. C., Chiaverini, J., La Rosa, J., & Miquel, J. C. (1995). Dyfamed, une station d'observation de l'environnement marin en Méditerranée. *Met. Mar.*, *167*, 33–36.

McClain, C. R., Esaias, W. E., Barnes, W., Guenther, B., Endres, D., Hooker, S., Mitchell, G., & Barnes, R. (1992). SeaWiFS calibration and validation plan. *NASA Technical Memorandum*, *3*.

McClain, C. R., & Fargion, G. S. (1999). SIMBIOS Project 1998 annual report. *NASA Technical Memorandum 1999-208645.* Greenbelt, MD: NASA Goddard Space Flight Center.

Moore, G. F., Aiken, J., & Lavender, S. J. (1999). The atmospheric correction of water color and the quantitative retrieval of suspended particulate matter in case II waters: application to MERIS. *International Journal of Remote Sensing*, *20*, 1713–1733.

Morel, A. (1974). Optical properties of pure water and sea water. In N. G. Jerlov, & E. Steemann-Nielsen (Eds.), *Optical aspects of oceanography* (pp. 1–24). London: Academic Press.

Morel, A. (1991). Light and marine photosynthesis: a spectral model with geochemical and climatological implications. *Progress in Oceanography*, *26*, 263–306.

Morel, A., & André, J.-M. (1991). Pigment distribution and primary production in the western Mediterranean as derived and modeled from Coastal Zone Color Scanner observations. *Journal of Geophysical Research*, *96*, 12685–12698.

Morel, A., & Antoine, D. (1994). Heating rate within the upper ocean in relation to its bio-optical state. *Journal of Physical Oceanography*, *24*, 1652–1665.

Morel, A., & Berthon, J.-F. (1989). Surface pigments, algal biomass profiles, and potential production of the euphotic layer: relationships reinvestigated in view of remote-sensing applications. *Limnology and Oceanography*, *34*, 1545–1562.

Moulin, C., Dulac, F., Lambert, C. E., Chazette, P., Janowiak, I., Chatenet, B., & Lavenu, F. (1997). Long-term daily monitoring of Saharan dust load over ocean using Meteosat ISCCP-B2 data: 2. Accuracy of the method and validation using Sun photometer measurements. *Journal of Geophysical Research*, *102*, 16959–16970.

Moulin, C., Guillard, F., Dulac, F., & Lambert, C. E. (1997). Long-term daily monitoring of Saharan dust load over ocean using Meteosat ISCCP-B2 data: 1. Methodology and preliminary results for 1983–1994 in the Mediterranean. *Journal of Geophysical Research*, *102*, 16947–16958.

Mueller, J. L., & Austin, R. W. (1995). Ocean optics protocols for SeaWiFS validation, revision 1. In S. B. Hooker, E. R. Firestone, & J.G Acker (Eds.), *SeaWiFS Technical Report Series, vol. 25. NASA Technical Memorandum 104566* (p. 67). Greenbelt, MD: NASA Goddard Space Flight Center.

Neckel, H., & Labs, D. (1984). The solar radiation between 3300 and 12500 A. *Solar Physics*, *90*, 205.

Neveux, J., & Panouse, M. (1987). Spectrofluorometric determination of chlorophylls and pheophytins. *Archive of Hydrobiology*, *109*, 561–567.

O'Reilly, J. E., Maritorena, S., Mitchell, B. G., Siegel, D. A., Carder, K. L., Garver, S. A., Kahru, M., & McClain, C. (1998). Ocean color chlorophyll algorithms for SeaWiFS. *Journal of Geophysical Research*, *103*, 24937–24953.

O'Reilly, J. E., Maritorena, S., Siegel, D., O'Brien, M. C., Toole, D., Mitchell, B. G., Kahru, M., Chavez, F. P., Strutton, P., Cota, G., Hooker, S. B., McClain, C. R., Carder, K. L., Muller-Karger, F., Harding, L., Magnuson, A., Phinney, D., Moore, G. F., Aiken, J., Arrigo, K. R., Letelier, R., & Culver, M. (2000). Ocean color chlorophyll a algorithms for SeaWiFS, OC2, and OC4: version 4. In S. B. Hooker, & E. R. Firestone (Eds.), *SeaWiFS Postlaunch Technical Report Series, vol. 11. SeaWiFS postlaunch calibration and validation analyses: part 3* (pp. 9–23). Greenbelt, MD: NASA Goddard Space Flight Center.

Prospero, J. M. (1996). Saharan dust transport over the North Atlantic Ocean and Mediterranean: an overview. In S. Guerzoni, & R. Chester (Eds.), *The impact of African dust across the Mediterranean* (pp. 133–152). Dordrecht, The Netherlands: Kluwer Academic Publishers.

Rabitti, S., Civitarese, G., & Ribera d'Alcalà, M. (1994). *Physical oceanography of the eastern Mediterranean (P.O.E.M.) data report: Part 2. Chemical and biological data.* Technical Report No. 13/94. Venice: Istituto di Biologia del Mare, CNR.

Rast, M., & Bezy, J. L. (1999). The ESA Medium Resolution Imaging Spectrometer MERIS a review of the instrument and its mission. *International Journal of Remote Sensing*, *20*, 1681–1702.

Robarts, R. D., Zohary, T., Waiser, M. J., & Yacobi, Y. Z. (1996). Bacterial abundance, biomass, and production in relation to phytoplankton biomass in the Levantine Basin of the southeastern Mediterranean Sea. *Marine Ecology: Progress Series*, *137*, 273–281.

Robilliard, D., Chami, M., Fonlupt, C., & Santer, R. (2000). *Using genetic programming to tackle the ocean colour problem*. Monaco: OOXV (Ocean Optics XV).

Sathyendranath, S., Cota, G., Stuart, V., Maass, H., & Platt, T. (2001). Remote sensing of phytoplankton pigments: a comparison of empirical and theoretical approaches. *International Journal of Remote Sensing*, *22*, 249–273.

Sathyendranath, S., & Platt, T. (1988). The spectral irradiance field at the surface and in the interior of the ocean: a model for applications in oceanography and remote sensing J. *Geophysical Research*, *93*, 9270–9280.

Schiller, H., & Doerffer, R. (1999). Neural network for emulation of an inverse model operational derivation of Case II water properties from MERIS data. *International Journal of Remote Sensing*, *20*, 1735–1746.

Seritti, A., Russo, D., Santinelli, C., Nannicini, L., Murru, E., & Manca, B. B. (2000). Vertical distribution of DOC in the Ionian Sea. In *Ocean biogeochemistry: a new paradigm*. JGOFS open science conference, Bergen, Norway.

Siegel, D. A., Wang, M., Maritorena, S., & Robinson, W. (2000). Atmospheric correction of satellite ocean color imagery: the black pixel assumption. *Applied Optics*, *39*, 3582–3591.

Smith, R. C., & Baker, K. S. (1978). The bio-optical state of ocean waters and remote sensing. *Limnology and Oceanography*, *23*, 247–259.

Tyrrell, T., Holligan, P. M., & Mobley, C. D. (1999). Optical impacts of oceanic coccolithophore blooms. *Journal of Geophysical Research*, *104*, 3223–3241.

Wang, M. (2000). SeaWiFS atmospheric correction algorithm updates. In S. B. Hooker, & E. R. Firestone (Eds.), *The SeaWiFS Postlaunch Technical Report Series, vol. 9. NASA Technical Memorandum 2000-206892* (pp. 58–64). Greenbelt, MD: NASA Goddard Space Flight Center.

Yacobi, Y. Z., Zohary, T, Kress, N., Hecht, A., Robarts, R. D., Waiser, M., & Wood, A. M. (1995). Chlorophyll distribution throughout the southeastern Mediterranean in relation to the physical structure of the water mass. *Journal of Marine System*, *6*, 179–190.

Yentsch, C. S. (1993). CZCS: its role in the study of the growth of oceanic phytoplankton. In V. Barale, & P. M. Schlittenhardt (Eds.), *Ocean colour: theory and applications in a decade of CZCS experience* (pp. 17–32). Dordrecht, The Netherlands: Kluwer Academic Publishers.

Yoder, J. A., McClain, C. R., Feldman, G. C., & Esaias, W. (1993). Annual cycles of phytoplankton chlorophyll concentrations in the global ocean: a satellite view. *Global Biogeochemical Cycles*, *7*, 181–193.